

INVESTIGATION OF BOILING HEAT EXCHANGE UNDER CONDITIONS SIMULATING WEAK GRAVITATIONAL FIELDS

Yu. A. Kirichenko, A. I. Charkin,
I. V. Lipamova, and V. L. Polunin

UDC 536.423.1

A method for simulating weak gravitational fields is presented; it is based on compensation of the gravitational force by a force acting on a magnetic liquid in an inhomogeneous magnetic field. Results are reported for an investigation of boiling heat exchange and the first critical heat flux under the conditions of weak gravitational fields.

The first investigations of boiling heat exchange under the conditions of weak gravitational fields were published at the end of the fifties [1]. Most of the work done since then has been carried out in free-falling containers or on board aircraft flying along a parabolic path [1-5].

In all cases, the test duration during "weightlessness" amounted to several seconds; the accuracy with which the state was realized did not exceed $\pm(0.01-0.03)g_n$. Lyon et al. [6] studied the relationship between the first critical heat flux and the gravitational acceleration for oxygen for long-term simulation of weak gravitational fields in the inhomogeneous magnetic field of a solenoid.

In our study, the source of the inhomogeneous magnetic field was a dc magnet with vertical gap, provided with magnetic poles of special configuration. As we shall show, our method of investigating boiling under conditions simulating weak gravitational fields offers certain advantages over the approach used in [6].

1. In simulation of weak gravitational fields and weightlessness, the magnetic-field configuration should be such that an identical force, compensating the force of gravity, acts on each elementary volume of the investigated fluid. Weightlessness is simulated by complete compensation, and weak gravitational fields by partial compensation.

Using the equation for the force acting on unit volume of a magnetic material in a magnetic field [7] and assuming that the density of the volume current is zero, while there is no pressure gradient, we obtain

$$f = -\frac{\chi}{2} \text{grad } H^2. \quad (1)$$

Introducing the load factor $\eta = g/g_n$, representing the relative simulated acceleration, we obtain

$$\eta = 1 - \frac{\chi}{2g_n} \text{grad } H^2. \quad (2)$$

We can simulate small load factors ($\eta < 1$) by creating a magnetic field with a constant value of $\text{grad } H^2$. Solenoids [6] or magnets [8-10] can be used. We employed a magnet with vertical gap, as being the most convenient for accommodation of the equipment and performance of the experiments (particularly those involving visual observations). The pole pieces were designed so as to maintain a constant value of $\text{grad } H^2 = 2HdH/dx$ in the plane of symmetry and an inverse proportionality between the magnetic field strength gap size, $H \sim 1/2z_0$ [10]. The pole profiles, asymptotically approaching the x and z axes, had the pole-piece diameter as limits (Fig. 1).

Low-Temperature Engineering-Physics Institute, Academy of Sciences of the Ukrainian SSR, Kharkov. Translated from *Inzhenerno-Fizicheskii Zhurnal*, Vol. 17, No. 2, pp. 201-209, August, 1969. Original article submitted October 2, 1968.

© 1972 Consultants Bureau, a division of Plenum Publishing Corporation, 227 West 17th Street, New York, N. Y. 10011. All rights reserved. This article cannot be reproduced for any purpose whatsoever without permission of the publisher. A copy of this article is available from the publisher for \$15.00.

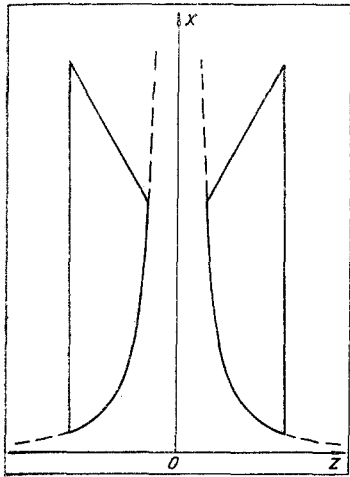


Fig. 1. Profile of pole pieces.

2. Figure 2 shows the experimental setup. A type SP-54 dc magnet with pole-piece diameter of 200 mm was used. The maximum field strength for simulation purposes was about 10^4 Oe for the minimum gap of 30 mm (Fig. 1).

The magnet was supplied by a 10 kW dc generator, controlled by means of the field-winding circuit. A type BT-4 regulator held field deviations within $\pm 0.01\%$. The magnetic field is measured by nuclear-resonance nutation of tap water with the aid of a nutation sensor with an effective dimension of 0.35 mm along the field gradient.

At each point in space where the condition $\text{grad} H^2 = \text{const}$ was satisfied, the magnetic-field measurement error was 0.03%. In the course of the experiment, the magnetic field was monitored by a type IMI-3 induction gauge, whose sensor was installed within the region of maximum magnetic field strength.

The investigated fluid (liquid oxygen) was contained within a glass Dewar vessel, located between the magnet poles. The heater, which also served as a resistance thermometer, was a 0.1 mm platinum wire, about 12 mm long. The thermometer was calculated by the method of [11]. The heater was supplied from a controllable regulated dc source.

The boiling curves showing the temperature difference (Δt as a function of the heat-flux density q) were obtained by measuring the resistance of the heater with an R-329 single-double bridge, and the current through the heater by a class 0.2 type M1108 ammeter. The critical heat flows were investigated in separate experiments; the onset of the crisis was detected from the jump exhibited by the need of an M-82 millivoltmeter. The error in measurement of the temperature was ± 0.1 deg, and in measurement of the heat flux density, $\pm 0.5\%$.

3. The lower limit to the load factors attainable was determined by several errors introduced by the characteristics of the simulation method. Let us first look at the error in realization of small load factors for a liquid of homogeneous temperature.

The condition requiring constancy of $\text{grad} H^2$ is only satisfied for the plane of symmetry of the magnet gap. As the distance from the plane of symmetry increases, the force components f begin to act [10]. It can be shown that for the volume of liquid bounded by the x_1 , x_2 , $+z$, and $-z$ coordinates, this will lead to an average error of

$$\Delta \eta_1 = \pm \frac{\sqrt{2}}{6} \frac{z^2}{x^2}, \quad (3)$$

where $x = (x_1 + x_2)/2$.

The precise manufacturing of the pole pieces introduces an error

$$\Delta \eta_2 = \pm 2 \left(\frac{\Delta x^2}{4x^2} + \frac{\Delta z^2}{z_0^2} \right)^{1/2}, \quad (4)$$

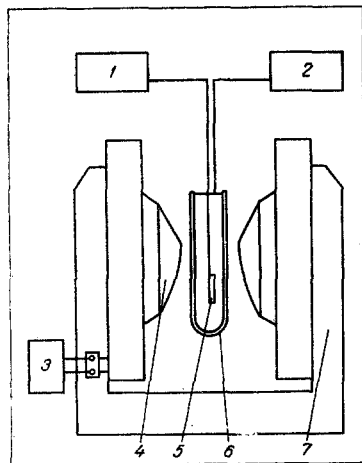


Fig. 2. Block diagram of experimental setup: 1) regulated controllable heater power supply; 2) magnetic field strength meter; 3) regulated controllable magnet power supply; 4) pole pieces; 5) platinum wire heater; 6) Dewar vessel; 7) dc magnet.

where Δx , Δz are the corresponding errors for the x and z axes. We obtain a formula of similar appearance for the error $\Delta\eta_3$ caused by inaccurate positioning of the pole pieces.

The error resulting from the change in the field when the investigated liquid is introduced is

$$\Delta\eta_4 = 2N\kappa, \quad (5)$$

where N is the demagnetization factor.

The error introduced by inaccurate regulation and measurement of the magnetic field can be estimated as

$$\Delta\eta_5 = \pm 2\Delta H/H. \quad (6)$$

The resultant error obtained by mean-square combination of all the above errors is

$$\Delta\eta = \sqrt{\sum_{i=1}^5 \Delta\eta_i^2} = \pm 0.004. \quad (7)$$

Here $x \approx 7$ cm, $z \approx 0.5$ cm, $z_0 \approx 2$ cm, $\Delta x = \Delta z = \pm 0.002$ cm, $\Delta H \approx \pm 10$ Oe.

The errors introduced by inaccurate determination of the specific magnetic susceptibility is

$$\Delta\eta_\chi = \Delta\chi/\chi \quad (8)$$

while for the temperature it is

$$\Delta\eta_T = \pm \frac{\Delta T}{T + \tilde{\Theta}} \approx \pm 0.007 \Delta T; \quad (9)$$

these do not affect satisfaction of the condition $\text{grad}H^2 = \text{const}$, and can be compensated by establishing the weightless state in terms of neutral equilibrium of a vapor bubble (see §6). In deriving (9), we took account of the relationship between the specific magnetic susceptibility χ and the temperature [12],

$$\chi = \frac{C}{T - \tilde{\Theta}}, \quad (10)$$

where C is a constant, and $\tilde{\Theta}$ is the Curie-Weiss point ($\tilde{\Theta} \approx 45^\circ\text{K}$ for oxygen).

4. In the study of heat exchange, additional errors are introduced by the temperature gradient in the fluid near the heater and by the appearance of vapor bubbles. By analogy with the thermal-convection solution, consideration of the mixed thermomagnetic and thermal convections leads to the relationship

$$\text{Nu} = C \text{Pr}^{0.25} (A + \text{Gr})^{0.25}, \quad (11)$$

where

$$\text{Gr} = \frac{\eta g_n \beta (T - \bar{T}) L^3}{\nu^2}; \quad A = \frac{(1 - \eta) g_n l^3 (T - \bar{T})}{\nu^2 (T + \tilde{\Theta})}.$$

From (11) we have

$$\text{Nu} = \text{Nu}_n \left[\eta + \frac{1 - \eta}{(T + \tilde{\Theta}) \beta} \right]^{0.25}, \quad (12)$$

where Nu_n is the Nusselt number for $\eta = 1$.

Relationship (12) indicates that the resultant heat-exchange coefficient for mixed thermal and thermomagnetic convection increases as η decreases. For oxygen, $(T + \tilde{\Theta})\beta \approx 0.58$, while when $\eta = 0$, $\text{Nu} \approx 1.15 \text{Nu}_n$.

Thus it is impossible to investigate the way in which convective heat exchange depends upon gravitational acceleration in simulation of small load factors in an inhomogeneous magnetic field.

5. Let us evaluate the influence of thermomagnetic convection on developed nucleate boiling. When the fluid near the heater becomes superheated, the relationship between the magnetic susceptibility and the temperature produces an uncompensated force f_m that acts on unit volume of fluid. We can assume that

f_m will intensify boiling, as it acts on the fluid volume V_m included between a vapor bubble and the heater surface. Boiling can be investigated in the case in which

$$f_m V_m < f_g V_b, \quad (13)$$

where $f_g \approx g_n \eta \rho$ is the buoyancy per unit volume of vapor bubble; $V_b = 4\pi R_0^3/3$ is the bubble volume.

Using (1), (2), and (10), we obtain

$$f_m = \frac{(1-\eta) g_n \rho \Delta t}{T + \bar{\Theta}}. \quad (14)$$

From (13) and (14) we obtain an estimate for the limiting simulated load factor,

$$\eta_{\text{lim}} > \frac{\Delta t}{T + \bar{\Theta}} \frac{V_m}{V_b}. \quad (15)$$

Let us estimate the value of η_{lim} for our study and for [6]. For us, $V_{1m} \approx R_0^2 b/2$, $b \approx 10^{-2}$ cm is the width of the heater, $V_{1m}/V_b \approx 5 \cdot 10^{-4}$, $\eta_{1\text{lim}} > 5 \cdot 10^{-4}$. For [6], $V_{2m} = R_0^3$, $V_{2m}/V_b \approx 0.25$, $\eta_{2\text{lim}} > 2 \cdot 10^{-2}$. In both cases, a value $\Delta t = 10^\circ$ was taken.

These estimates show that thin heaters offer definite advantages. For a heater with developed surface (of the order of the separation diameter of a bubble, or more) the limiting load factors for which boiling can be studied will in all cases exceed several hundredths of g_n .

6. Under simulation conditions, various load factors will act on vapor bubbles and on the liquids during boiling. Determining the apparent load factor η'' for bubbles in terms of the bubble buoyancy under simulation conditions, we obtain

$$\eta'' = 1 - \frac{\kappa - \kappa''}{2g_n(\rho - \rho'')} |\text{grad } H^2|. \quad (16)$$

Determining $\text{grad } H^2$ in terms of (2) for sufficiently small η we have

$$\eta'' = \eta + \frac{\rho''}{\rho - \rho''} \left(\frac{\kappa''}{\kappa} - 1 \right). \quad (17)$$

Substituting the numerical values for oxygen at 90°K into this gives

$$\eta'' = \eta + 1.9 \cdot 10^{-3}. \quad (18)$$

In simulation of weightlessness for oxygen, a buoyancy corresponding to a gravitational force $g = g_n \eta'' = 1.9 \cdot 10^{-3}$ will act on the bubbles.

The negligible difference between η and η'' permits reliable determination of the instant at which weightlessness sets in on the basis of the neutral equilibrium of the bubbles. The small increase in gravitational convection is of no great importance in view of the strong thermomagnetic convection at low load factors.

The possibility of exactly recording the instant at which the weightless state occurs is one of the major advantages of our method, permitting visual observation of the process under study.

Summing all the error sources considered, we conclude that it is possible to simulate weak gravitational fields in a study of boiling, with an accuracy of the order of $\Delta\eta = \pm 0.005$.

7. Heat exchange in bubble boiling was studied for several simulated values of gravitational acceleration.

Figure 3 shows the average relationships between the heat-exchange coefficient α and the heat-flux density q for several values of η . For convective heat exchange at low load factors ($\eta = 0.05-0.3$), the heat-exchange coefficient is greater than under normal conditions ($\eta = 1$), owing to the strong influence of thermomagnetic convection (see §5). For developed nucleate boiling, the curves for load factors greater than $\eta = 0.04$ nearly coincide. (As we have indicated, the influence of thermomagnetic convection is negligible in this case.) For load factors less than $\eta = 0.04$, there is almost no region of developed nucleate boiling; the region is restricted to low values of critical heat flux.

TABLE 1. Parameters for Nucleate Boiling of Liquid Oxygen under Weak Gravitational Field Conditions

Expt. No.	η	$\alpha \cdot 10^{-4}$	k	Expt. No.	η	$\alpha \cdot 10^{-4}$	k
1	0,04	4,4	0,9	11	0,3	4,4	0,88
2	0,04	3,4	0,88	12	0,3	4,9	0,7
3	0,05	3,85	0,85	13	0,5	3,8	0,82
4	0,05	3,4	0,92	14	0,5	4,5	0,7
5	0,05	3,7	0,83	15	0,65	4,2	0,79
6	0,05	4,8	0,86	16	1	4,3	0,77
7	0,1	3,4	0,88	17	1	3,7	0,8
8	0,1	4,3	0,83	18	1	3,8	0,8
9	0,1	4,5	0,78	19	1	3,1	0,78
10	0,1	4,7	0,88	20	1	3,8	0,88

Note: Average value, 4.0 ± 0.5 , 0.82 ± 0.06 .

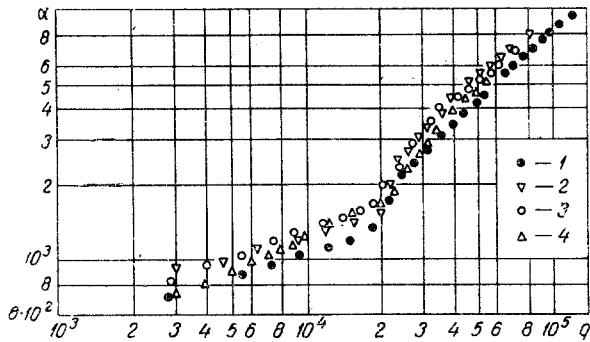


Fig. 3. Curves for boiling of liquid oxygen at various load factors (α , $W/m^2 \cdot \text{deg}$; q , W/m^2). Values of η : 1) 1; 2) 0.3; 3) 0.1; 4) 0.05.

Agreement has been obtained between the heat-exchange coefficient for $g = g_n$ and for "weightlessness," realized to within $\pm(0.01-0.03)q_n$ [2, 5].

In visual observation of the boiling process, it was found that the rate of bubble ascent decreased and the separation diameter increased as the simulated load factors decreased. When $\eta = 0$, vapor bubbles did not separate from the heater, but combined to form a void, which gradually enveloped the entire heater.

8. Figure 4 shows the critical heat flux q_* of a function of g in relative units. When $\eta = 1$, i.e., in the absence of the field, the average critical heat flux is $\bar{q}_* = (119,000 \pm 3600) W/m^2$.

Table 2 shows q_* data at weightlessness for two different heaters. The average value was based on the mean-square error of several measurements.

Processing of the data for the critical heat flux (147 separate measurements) yielded the relationship

$$\frac{q_*}{q_{*n}} = \left(\frac{g}{g_n} \right)^k, \quad k = 0.26 \pm 0.01. \quad (20)$$

The data obtained confirm that the Kutateladze-Zuber hydrodynamic theory of crises can be used for small gravitational acceleration ($0.01 < \eta < 1$) [13, 14].

Figure 4 also gives published data obtained under free-fall conditions [2, 3] and in simulation of "weightlessness" in the magnetic field of a solenoid [6]. The results of the very careful work of Merte and Clark [2] coincide with ours to a load factor of $\eta = 0.03$, which corresponds to the accuracy of simulation attained in [2].

The values obtained by Usiskin and Siegel are too high; these authors themselves explain this in terms of the characteristics of their method and by the short time over which the experiments were conducted (about 1 sec). The anomalously weak dependence of q_* on η found in [6] for $\eta < 0.3$ can most likely be explained by the very strong influence of thermomagnetic convection.

TABLE 2. Critical Heat Fluxes for Liquid Oxygen under Conditions Simulating Weightlessness

Heater number	Experiment number	$q_* \cdot 10^{-4}$, W/m ² · deg	Heater number	Experiment number	$q_* \cdot 10^{-4}$, W/m ² · deg
1	1	2,73	2	1	2,62
	2	2,82		2	2,80
	3	2,88		3	2,83
	4	3,13		4	2,47
	5	2,90		5	3,11
	6	3,04		6	3,04
Average value		2,86 ± 0,19	Average value		2,86 ± 0,19

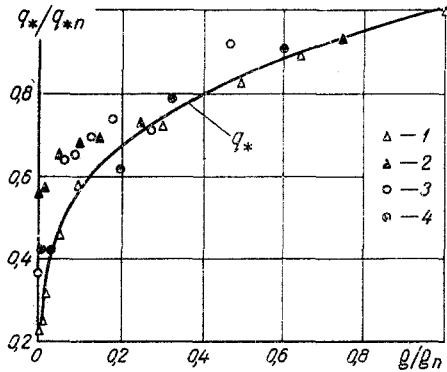


Fig. 4. Relative critical heat flux as function of load factor ($q_* = q_{*n} \cdot (g/g_n)^{0.25}$): 1) experimental data of authors; 2) data of Lyon [6]; 3) data of Usiskin and Siegel [3]; 4) data of Merte and Clark [2].

Some idea as to the accuracy with which the weightless state was realized for each of the given studies can be obtained by calculating the value of η that corresponds to the ratio q_*/q_{*n} obtained for $\eta = 0$. Calculations based on (7) yield the following: for [2], $\eta = 0.02$; for [3], $\eta = 0.03$; for [6], $\eta = 0.1$; for our study, $\eta = 0.003$. The last value is comparable with the load factor by which "weightlessness" differs from the liquid and the vapor.

Our simulation method is also suitable for investigating the growth and motion dynamics of vapor and gas bubbles in weak gravitational fields. There may be another interesting application of the method after it has been refined somewhat: the study of the physical properties of oxygen near the critical (thermodynamic) point under conditions of weightlessness.

The results obtained will not be distorted by the gravitational effect that ordinarily occurs near the critical point owing to a sharp increase in compressibility.

NOTATION

- g is the simulated gravitational acceleration;
- g_n is the normal gravitational acceleration, $g_n = 9.81 \text{ m/sec}^2$;
- ρ is the density of the liquid;
- ρ'' is the density of the vapor;
- x is the magnetic susceptibility;
- μ is the magnetic permeability;
- $\chi = x/\rho$ is the specific magnetic susceptibility of the liquid;
- χ'' is the specific magnetic susceptibility of the vapor;
- η is the load factor, $\eta = g/g_n$;
- η'' is the load factor for vapor;
- H is the magnetic field strength;
- H_0 is the magnetic field strength corresponding to $\eta = 0$;
- x, z are Cartesian coordinates;
- $2z_0$ is the magnet gap;
- T is the temperature;
- \bar{T} is the mean-volume temperature of the liquid;
- Θ is the Curie-Weiss point for oxygen;
- β is the coefficient of volume expansion;
- V_m is the volume of liquid included between heater and bubble;
- V_b is the volume of the vapor bubble;
- R_0 is the radius of the vapor bubble at separation from the heater;
- f is the force acting on unit volume of the fluid
- $f = g_n \eta \rho$;
- f_m is the force produced by the difference χ ;
- q is the heat flux density;
- q_* is the value of the first critical heat flux.

LITERATURE CITED

1. R. Siegel and C. Usiskin, *Trans. ASME, Ser. C, Heat Transfer*, 81, No. 3, 230 (1959).
2. H. Merte and J. Clark, *Trans. ASME, Ser. C, Heat Transfer*, 86, No. 3, 66 (1964).
3. C. Usiskin and R. Siegel, "Experimental investigation of boiling under reduced and zero gravity," in: *Weightlessness [Russian translation]*, Mir, Moscow (1964), p. 103.
4. G. Steinle, "Experimental investigation of transition from nucleate to film boiling in weightless state," in: *Weightlessness [Russian translation]*, Mir, Moscow (1964), p. 149.
5. J. E. Sherly, *Advances in Cryogenic Engineering*, Vol. 8, Plenum Press, New York (1963).
6. D. N. Lyon, M. C. Jones, G. L. Ritter, C. J. Chiladacis, and P. G. Kosky, *AIChE J.*, 11, No. 5, 773 (1965).
7. L. D. Landau and E. M. Lifshits, *Electrodynamics of Continuous Media [in Russian]*, GITTL, Moscow (1957).
8. R. A. Fereday, *Proc. Phys. Soc.*, 42, Part 3, No. 233, 251 (1930).
9. N. Davy, *Phil. Mag.*, 33, No. 233, 575 (1942).
10. M. Garber, W. Henry, and H. Hoeve, *Canad. J. Phys.*, 38, No. 12, 1595 (1960).
11. A. D. Brodskii, *New Methods for Measuring Low Temperatures [in Russian]*, Standartgiz, Moscow (1962).
12. Ya. G. Dorfman, *Magnetic Properties and Structure of Matter [in Russian]*, GITTL, Moscow (1955).
13. S. S. Kutateladze, *Chur. Tekh. Fiz.*, 20, No. 11 (1950).
14. G. Leppert and C. Pitts, "Boiling," in: *Problems of Heat Exchange [Russian translation]*, Atomizdat, Moscow (1967), p. 142.